microbial biotechnology

Open Access

Field detection of urease and carbonic anhydrase activity using rapid and economical tests to assess microbially induced carbonate precipitation

Fernando Medina Ferrer,[1] Kathryn Hobart[1,2] and Jake V. Bailey[1]*

[1]*Department of Earth & Environmental Sciences, College of Science & Engineering, University of Minnesota, Twin Cities, Minneapolis, MN, USA.*

[2]*Institute for Rock Magnetism, University of Minnesota, Twin Cities, Minneapolis, MN, USA.*

Summary

Microbial precipitation of calcium carbonate is a widespread environmental phenomenon that has diverse engineering applications, from building and soil restoration to carbon sequestration. Urease-mediated ureolysis and CO_2 (de)hydration by carbonic anhydrase (CA) are known for their potential to precipitate carbonate minerals, yet many environmental microbial community studies rely on marker gene or metagenomic approaches that are unable to determine *in situ* activity. Here, we developed fast and cost-effective tests for the field detection of urease and CA activity using pH-sensitive strips inside microcentrifuge tubes that change colour in response to the reaction products of urease (NH_3) and CA (CO_2). The urease assay proved sensitive and useful in the field to detect *in situ* activity in biofilms from a saline lake, a series of calcareous fens, and ferrous springs, finding relatively high urease activity in lake samples. Incubations of lake microbes with urea resulted in significantly higher $CaCO_3$ precipitation compared to incubations with a urease inhibitor, showing that the rapid assay indicated an on-site active metabolism potentially mediating carbonate precipitation. The CA assay, however, showed less sensitivity compared to the urease test. While its sensitivity limits its utility, the assay may still be useful as a preliminary indicator given the paucity of other means for detecting CA activity in the field. Field urease, and potentially CA, activity assays complement molecular approaches and facilitate the search for carbonate-precipitating microbes and their *in situ* activity, which could be applied toward agriculture, engineering and carbon sequestration technologies.

Received 30 March, 2020; accepted 26 June, 2020.
*For correspondence. E-mail baileyj@umn.edu;
Tel. +1 612 624 1603; Fax +1 612 625 3819.
Microbial Biotechnology (2020) **13**(6), 1877–1888
doi:10.1111/1751-7915.13630
Funding information
This research was funded by a NASA award NNX14AK20G to JVB. FMF acknowledges the UMN Graduate School DDF, Fulbright 15150776 and CONICYT folio-72160214 fellowships. KH was supported by a MnDRIVE Environment initiative grant at the University of Minnesota.

Introduction

Microbially induced calcium carbonate precipitation (MICP) is a widespread environmental process that affects the carbon cycle and that has been explored as an alternative solution for several engineering and environmental challenges, such as restoration of concrete structures, soil consolidation, pollutant bioremediation and CO_2 sequestration (Sarayu *et al.*, 2014; Li *et al.*, 2015; Bose and Satyanarayana, 2017; Krajewska, 2018; Reeksting *et al.*, 2020). Despite its environmental relevance and multiple applications, MICP can be difficult to assess and identify in a given environment. Current environmental microbiota analyses commonly characterize communities via 16S rRNA gene sequencing and metagenomic sequencing. High-throughput sequencing techniques, however, fail to determine active metabolisms, unless they are complemented with challenging and labour-intense transcriptomic or culture-based analysis, which do not necessarily reflect *in situ* activity. It is possible, however, to directly test the activity of certain enzymes in the field and identify active metabolisms on-site, therefore, assessing the microbial function in a particular environment. Here, we developed a method for the field detection of urease (EC 3.5.1.5) and carbonic anhydrase (CA; EC 4.2.1.1) activity, two enzymes associated with MICP (Achal and Pan, 2011), to reveal microbial communities that potentially promote carbonate precipitation *in situ*.

Metabolisms such as photosynthesis, methane oxidation, nitrate reduction, bicarbonate transport and ureolysis can locally increase carbonate saturation and promote MICP (Zhu and Dittrich, 2016; Seifan and Berenjian, 2019). Two of these metabolisms rely on enzymes whose activity can potentially be detected in

the field: ureolysis and CO_2 (de)hydration via CA. Ureolysis, catalysed by urease, allows microorganisms to use urea as a nitrogen and carbon source (Krausfeldt *et al*., 2019). CA facilitates rapid carbon transport into the cell via CO_2-HCO_3^- interconversion (Kumar and Ferry, 2014). Both enzymes generate carbonate anions and increase the pH as a product of their activity. Urease generates ammonia and CO_2 from urea (Eq. 1), which coupled to ammonia hydrolysis and CO_2 hydration, a reversible reaction catalysed by CA (Eq. 2), produces one mol of hydroxide and one mol of bicarbonate per mol of urea (Eq. 3):

$$(NH_2)_2CO_{(aq)} + H_2O_{(l)} \rightarrow CO_{2(g)} + 2NH_{3(g)} \quad (1)$$

$$CO_{2(g)} + H_2O_{(l)} \rightleftharpoons HCO^-_{3(aq)} + H^+_{(aq)} \quad (2)$$

$$(NH_2)_2CO_{(aq)} + 3H_2O_{(l)} \rightarrow HCO^-_{3(aq)} + 2NH^+_{4(aq)} + OH^-_{(aq)} \quad (3)$$

The production of hydroxide and bicarbonate increases the saturation state with respect to calcium carbonates, promoting their precipitation. Urease and CA have been shown to drive MICP in multiple environments (Dhami *et al*., 2013; Seifan and Berenjian, 2019), yet their effects are commonly evaluated via culture-based approaches, disregarding the activity of complex communities *in situ*. An alternative approach is to test the enzymatic activity from microbial biofilms directly in the field. Existing urease and CA assays, however, are not efficient for field testing. For example, ammonia detection by the Berthelot reaction is commonly used to evaluate urease activity by a colour change in solution (e.g. Kandeler and Gerber, 1988; Sinsabaugh *et al*., 2000; Cordero *et al*., 2019), which is dramatically affected by the inherent components of environmental samples (e.g. pigments in photosynthetic biofilms preclude the reading of the assayed solutions), requiring high sample dilution, several individual steps, long incubation times and laboratory equipment, which prevent its application in the field. In the case of CA, most activity measurements are dependent on a solution-based colorimetry of its esterase activity (e.g. Baliukynas *et al*., 2020), a characteristic known to only some CA isoforms from few organisms (Innocenti and Supuran, 2010). Methods that instead evaluate the CA hydratase activity are based on a pH change in solution, which could also be affected by the inherent buffering capacity of environmental samples. These urease and CA assays were intended to evaluate the enzymatic activity from protein extracts of cultured organisms or from laboratory-processed samples, rather than complex environmental samples, and cannot be implemented in the field without sophisticated equipment. To circumvent these inconveniences, we used a pH-sensitive strip to detect the gaseous products of urease and CA reactions, NH_3 and CO_2, respectively, which diffuse from the enzymatic reaction site and can therefore be detected with minimal interference from other components of an aqueous environmental sample. Separating the gas detection site from the enzymatic reaction site can be achieved inside a microcentrifuge tube, which makes the tests suitable for field deployment. We evaluated on-site urease and CA activities using this strategy in samples from calcareous fens, iron-rich springs and a saline lake. In these settings, the environmental conditions may lead to carbonate precipitation; however, the contribution of MICP is difficult to assess in the absence of a field assay. By using a field test, we obtained a preliminary assessment of potential MICP, which can be applied to identify environments with relevant microbial carbonate mineralization, and to facilitate the management of urease- and CA-based technologies.

Results and discussion

Rapid test sensitivity and reproducibility

A pH-sensitive dye encapsulated within a cellulose matrix was used as a detector of NH_3 or CO_2 inside the cap of microcentrifuge tubes. Urease activity was followed by an ammonia-mediated pH increase, whereas CA was detected by a CO_2-driven pH decrease. The urease test, described in the Experimental procedures section and in Figure 1A–C, turns a phenol red indicator from yellow to red in less than 15 min when > 30 mU urease is assayed (Fig. 2A). The hues in the indicator are significantly affected by the incubation time ($F = 429.6$, DFn = 3.2, DFd = 125.8, $P < 0.0001$) and by the incubation condition ($F = 258.9$, DFn = 7, DFd = 40, $P < 0.0001$). After 30 min, the method sensitivity is ~ 3 mU when compared to a phenyl phosphorodiamidate (PPD)-containing negative control (Fig. 2B), which is comparable to the response using the Berthelot reaction in a canonical urease quantification assay (Fig. S1).

In contrast to the urease test, the CA assay (Fig. 1D–F) yields only a subtle colour change when compared to acetazolamide-containing negative controls, because the rapid and spontaneous bicarbonate dehydration, even without the enzyme, turns metacresol purple indicator to yellow within 30 min (Fig. 2C). Detection of the CA hydratase activity by any method, however, is limited by its fast non-enzymatic reaction, therefore always requiring a comparison with a negative control at a given reaction time. CA-containing assays show hues significantly affected by the incubation time ($F = 117$, DFn = 2.22, DFd = 93.2, $P < 0.0001$) and by the incubation condition ($F = 5.8$, DFn = 5, DFd = 42, $P = 0.0004$). Pairwise comparisons between conditions with and without inhibitor assayed simultaneously, however, show subtle hue differences, mostly significant ($P < 0.05$) at 15 nM CA or higher (Fig. 2

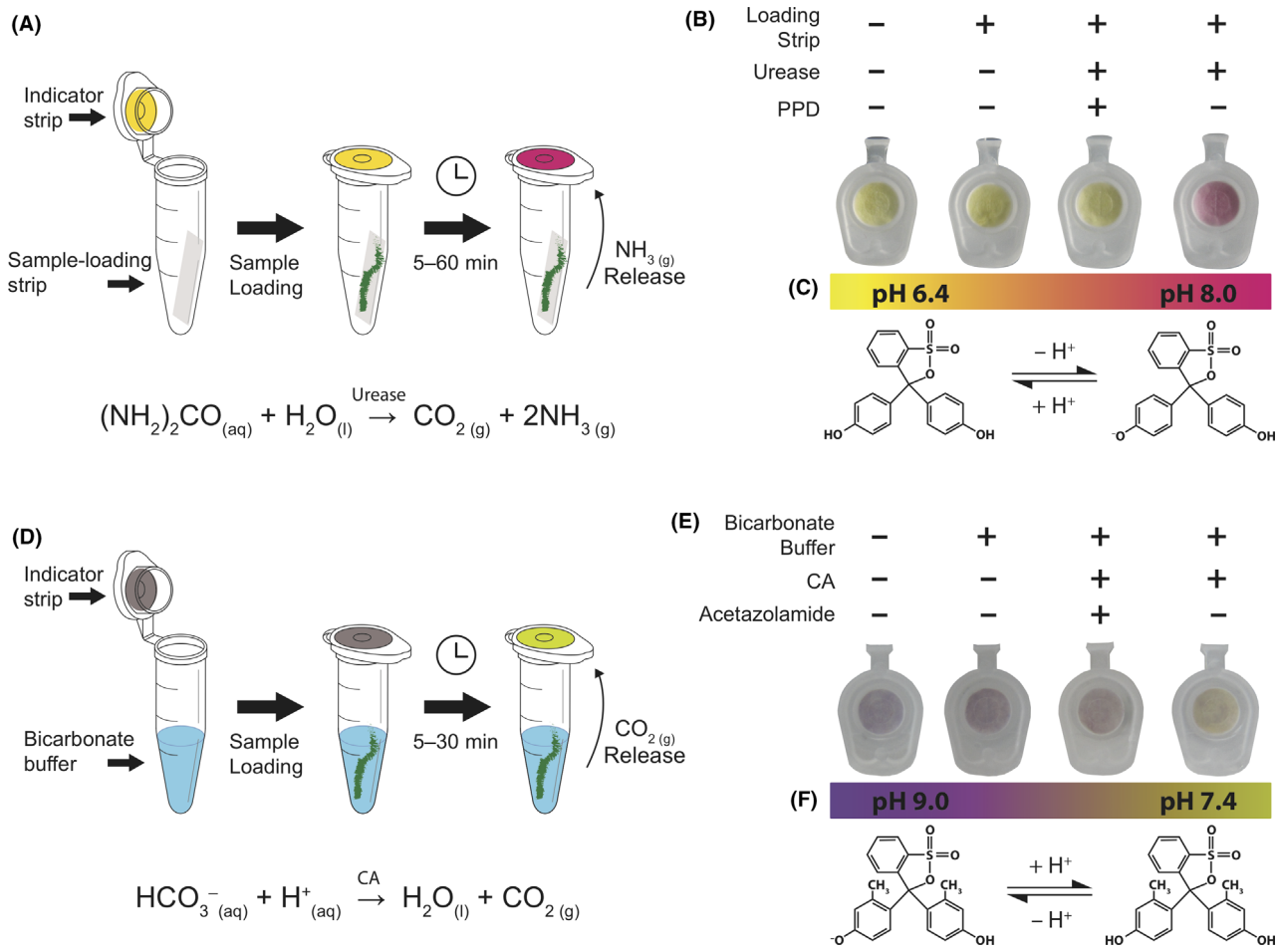

Fig. 1. Urease and CA field tests.
A. Representation of a positive urease assay after adding a biofilm sample in direct contact with the loading strip.
B. A switch to red in the tube cap (indicator strip) indicates a positive urease reaction. If no urease is present, or if a loading strip with urease inhibitor (PPD) is assayed, the indicator is expected to remain yellow.
C. Colour transition of phenol red (pKa 7.4, pH range 6.4–8.0) used for urease tests.
D. CA assay scheme after adding a sample in the tube with bicarbonate solution.
E. Faster development of a yellow colour in the indicator than a negative control (no sample added or using a CA inhibitor) indicates positive CA activity.
F. Colour transition of metacresol purple (pKa 8.32, pH range 7.4–9.0) used for CA assays.

D). By contrast, a canonical CA hydratase assay shows sensitivities as low as 0.15–0.3 nM CA (Fig. S1).

Field detection of urease and CA activity

Urease and CA tests were used for on-site enzymatic activity detection in samples from a saline lake, ponds from calcareous fens and iron oxide precipitates from ferrous springs (Figs S2–S5). Biomass collected during a bloom event in Salt Lake and a sample of green filaments collected after the bloom were urease-positive, where the incubation time significantly affected the hues ($F = 13.8$, DFn = 1.4, DFd = 2.8, $P = 0.036$, and; $F = 23$, DFn = 1.1, DFd = 4.4, $P = 0.0064$ respectively), and finding a significant difference ($P < 0.05$) in less than 35 min when compared to negative control assays (Fig. 3A and B).

Nicols Meadow Fen samples were also positive for urease, with hues significantly affected by the incubation time ($F = 13.3$, DFn = 1.2, DFd = 4.9, $P < 0.014$), although they showed less colour change intensity than the samples from Salt Lake (Fig. 3C and D). Green photosynthetic sheaths from Fortier-Sioux Nation Fen and green biofilms from Black Dog Lake Fen showed comparatively less urease activity, where the incubation time did not significantly affect their hues ($F = 3.4$, DFn = 1.1, DFd = 4.2, $P = 0.134$, and; $F = 4.3$, DFn = 1.1, DFd = 4.2, $P = 0.101$ respectively), despite showing a slight positive red coloration after one hour of incubation (Fig. 3C and D). In organisms that do not constitutively

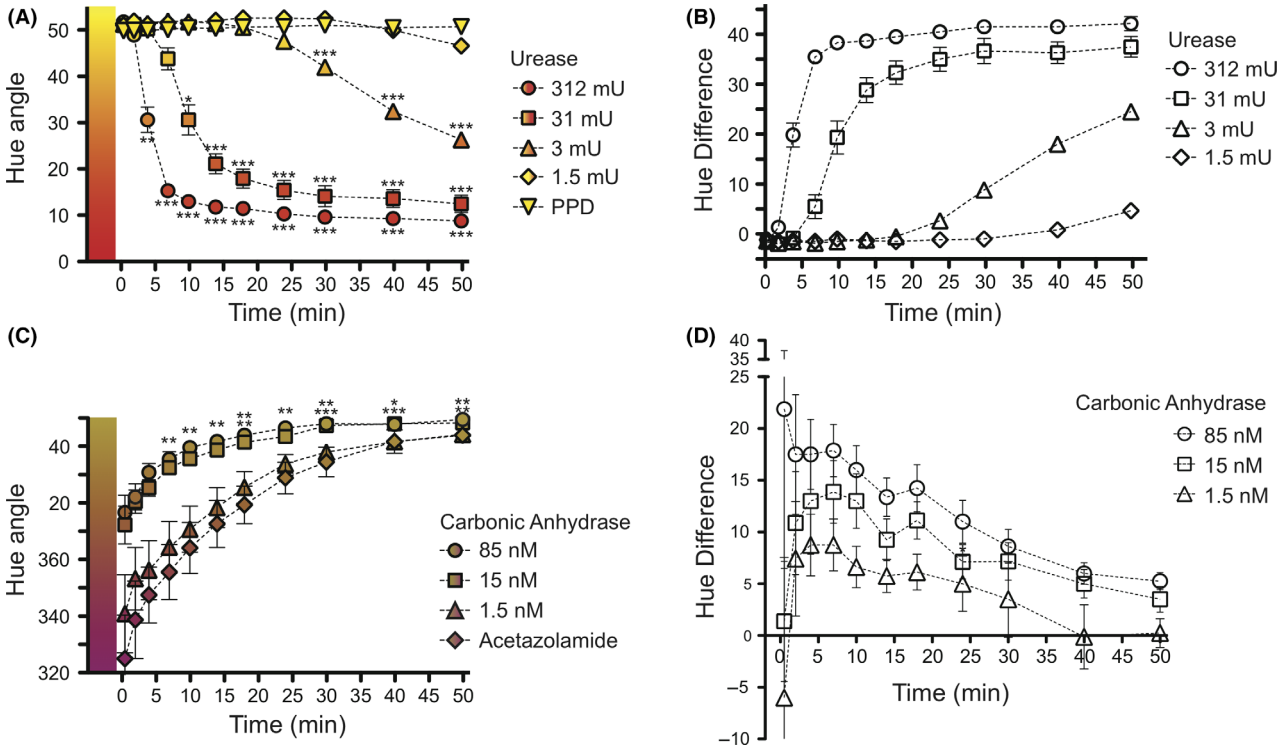

Fig. 2. Field test colour change kinetics and sensitivities.
A. Assay colour (expressed as average hue values) as a function of incubation time for the urease test using different urease standards (1.5–312 mU), and the average of their negative controls containing a urease inhibitor (PPD).
B. Hue difference of urease assays compared to their respective negative controls.
C. CA assay hue as a function of incubation time after adding different CA concentrations (1.5–85 nM), and the average of their negative controls in the presence of a CA inhibitor (acetazolamide).
D. Hue difference of CA standards compared to their respective negative controls. All conditions were assayed using six replicates. Error bars represent standard error (if not shown, the error is smaller than the symbols). *$0.1 < P < 0.05$, **$0.05 < P < 0.01$, ***$P < 0.01$ between each condition and its respective negative control assessed by Bonferroni's multiple comparisons test.

express urease, its expression is likely induced when urea is available (Mobley *et al*., 1995; Zhou *et al*., 2019). The higher urease activity in Salt Lake may therefore reflect urea accessibility and correlate with the bloom event observed in July 2019. Agriculture promotes eutrophication (Paerl *et al*., 2016), and in particular urea – the major worldwide fertilizer (Glibert *et al*., 2014) – can be used by microbes as both N and C source (Krausfeldt *et al*., 2019). Salt Lake is located in close proximity to farmland, and its microbial communities may be sensitive to nearby fertilization practices. By contrast, less urease activity found in calcareous fen samples, in particular Fortier-Sioux Nation Fen, which is located near a State Wildlife Management Area, may reflect a lower agriculture impact (Fig. S6).

Soudan seep biofilms showed slight urease-positive reactions with hues significantly influenced by the incubation time ($F = 6.05$, DFn = 1.6, DFd = 6.6, $P = 0.036$; Fig. 3E and F). Biofilms at St. Mary's Spring have a combination of green cyanobacterial filaments that were slightly positive for urease, with hues significantly affected by the incubation time ($F = 40.4$, DFn = 1.8, DFd = 7.2, $P = 0.0001$), and stalks of iron-oxidizing bacteria surrounded by few cyanobacteria and iron oxides, which were urease-negative (Fig. 3E and F). Iron oxides from Black Dog Lake North Fen creek were also urease-negative. PPD-containing controls in these ferric precipitates, however, showed a slight colour change (represented by low hues, and a negative hue difference in Fig. 3E and F), attributed to ammonia release from urea (which may be less stable in the presence of PPD) or from PPD degradation. The P–N bonds in phosphoramidates are unstable in aqueous solutions (Kafarski and Talma, 2018) and may release ammonia. Moderate transitions to red may lead to false positives, although its intensity was not comparable to the positive reactions observed in other environments. Several other urease inhibitors not tested in this study (Amtul *et al*., 2002) may prevent false positives; however, phosphoramidates (such as PPD) are among the most potent and specific urease inhibitors (Kafarski and Talma, 2018) and were therefore selected for this assay.

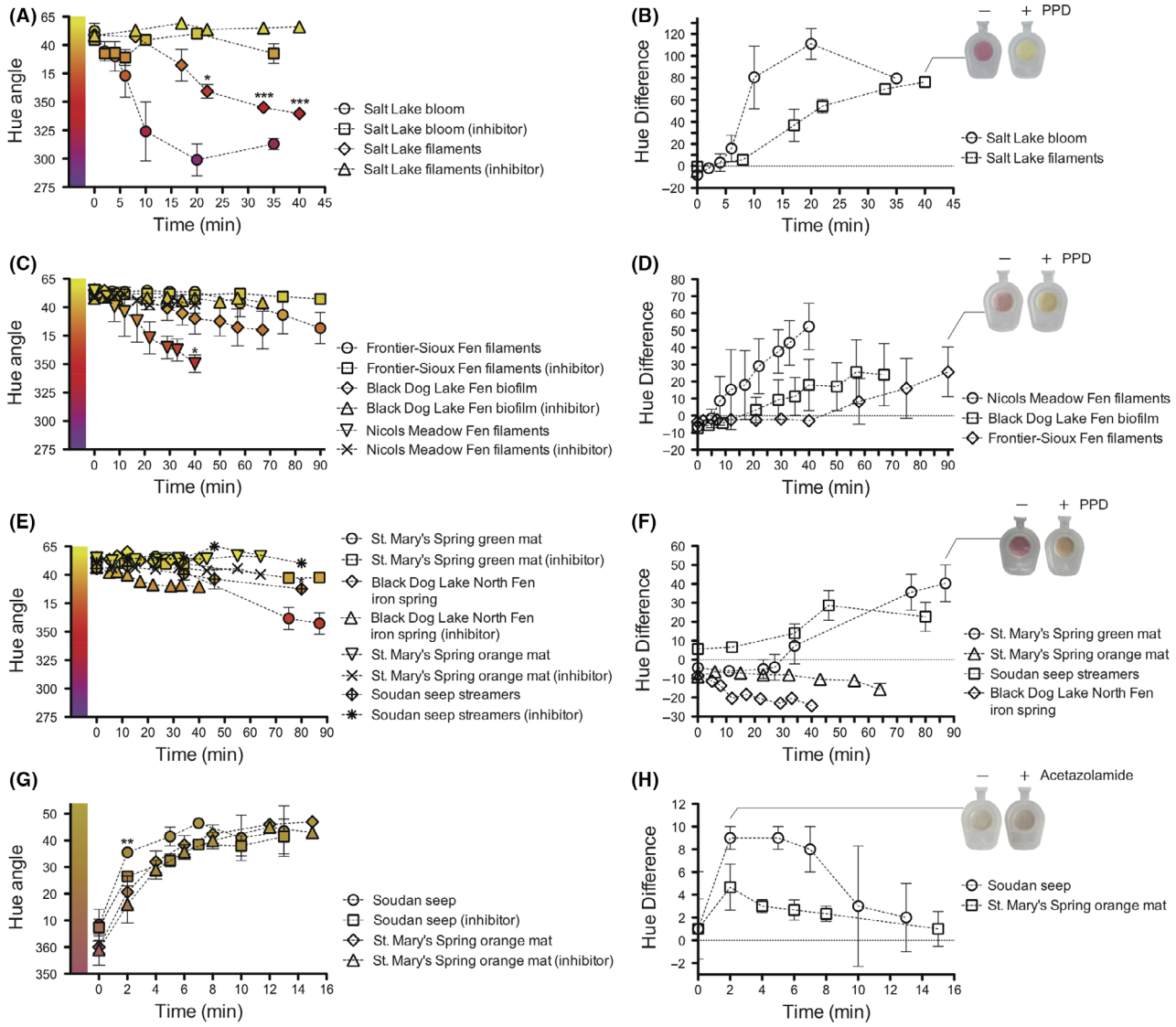

Fig. 3. Field test colour change using environmental samples. Hue, and hue difference from on-site urease assays compared to their respective negative controls of Salt Lake (A, B), calcareous fen (C, D) and iron spring (E, F) samples. CA assay hue (G) and hue difference (H) of ferric precipitates is also shown, along with representative pictures of tubes without (–) and with (+) inhibitors for particular time points and samples. When shown, error bars are larger than their respective symbols, representing the standard error. *$0.1 < P < 0.05$, **$0.05 < P < 0.01$, ***$P < 0.01$ between each sample and its respective negative control according to Bonferroni's multiple comparisons test.

In contrast to urease, the CA assay did not show colour differences in Salt Lake and calcareous fen samples. Only Soudan seep samples showed subtle visual differences compared to negative controls that were significant (Bonferroni-corrected P-value = 0.037) at 2 min of assay (Fig. 3G and H). It is generally expected to find CA in photosynthetic biofilms as part of their CO_2 concentrating mechanisms (Kumar and Ferry, 2014), and thus, CA levels in most analysed samples were possibly below the detection limit of the field assay. While the urease assay was shown to be robust and shown to have low detection limits, the CA assay was limited by the nature of its catalysed reaction (Eq. 2), which always requires a rigorous comparison with a negative control at a particular time. In addition, carbonic anhydrases include at least six enzyme classes with no structural or sequence homology and, consequently, the inhibitor choice may have varied effects. Although acetazolamide is a potent wide-spectrum CA inhibitor (Zimmerman et al., 2004, 2007), it is possible that certain microbial CA were not effectively inhibited, which would yield higher negative control rates and thus lower assay sensitivities when compared to conditions without inhibitors. We failed, however, to obtain environmental protein extracts with significant soluble CA

activity in the laboratory, using a conventional assay (Fig. S7), even in photosynthetic cells. We also found very low soluble urease activity from protein extracts (Fig. S7), indicating that most on-site activity found may have been the result of extracellular, possibly membrane bound or extracellular polymeric substances (EPS)-associated urease, which was observed as residual urease activity of cell debris after protein extraction.

The different factors affecting the quality of the CA field detection method (such as ice incubation, rigorous comparison with a negative control at a particular time, colour change of the detection strip with atmospheric CO_2 within days of storage and lower sensitivity compared to conventional laboratory assays) limits its reliable application in a field setting. To our knowledge, however, there are no reported CA assays for field detection, and thus, the strategy described here could provide preliminary semi-quantitative information of CA activity in the environment. The applicability of the field CA assay for environmental samples may be improved by using more sensitive and stable CO_2 detectors, along with negative controls containing a cocktail of different CA inhibitor types.

Carbonate precipitation induced by urease and CA

Differences in intensity and time to obtain a positive reaction serve as parameters to compare relative activities among sites, where the strongest urease activity was found in Salt Lake samples. To determine potential urease- and CA-dependent MICP, we incubated Salt Lake filaments with lake water containing urea, showing a significant decrease in its Ca^{2+} concentration (14.4 ± 0.5 mM) through time ($F = 118.8$, DFn = 4.1, DFd = 33.2, $P < 0.0001$) starting at Day 4 and depleting at Day 9 (Fig. 4A). The calcium drop is interpreted as calcium carbonate precipitation, which was also observed by the solution turbidity (attributable to $CaCO_3$) starting at Day 3–4 (Fig. 4B–D). By contrast, incubations in the presence of PPD depleted only around one-third of the initial calcium after 12 days, having significantly higher calcium than incubations without PPD after Day 4 (Fig. 4A).

Filament incubations in the presence of acetazolamide, however, did not prevent calcium depletion (Fig. 4). Therefore, urease, and not CA activity, is most likely responsible for carbonate precipitation under the studied conditions, consistent with the enzymatic activity observed in the field. Between Days 4 and 7, however, a delay in calcium depletion with acetazolamide compared to the condition without inhibitor may indicate a possible CA influence on $CaCO_3$ precipitation dynamics. Both enzymes may synergistically affect carbonate precipitation, as suggested previously (Dhami *et al*., 2014), via rapid bicarbonate generation by CA (Eq. 2) from CO_2 produced by urease (Eq. 1), providing CO_3^{2-} and neutralizing the acidity produced by CO_2 hydration. The mechanism by which urease promoted $CaCO_3$ precipitation is attributable to a pH increase during incubations compared to the lake water initial pH (Fig. 4A). Without PPD, the pH rises more than 0.5 units in 12 days, increasing the saturation with respect to carbonate minerals (Fig. S8).

Following 12 days, the filaments were covered by a white precipitate, extensively found in incubations without inhibitors or with acetazolamide only. Under the microscope, green trichomes were encrusted by precipitates, which appeared white under phase contrast, blackish under bright field, and were autofluorescent (Fig. 5A). The encrusting particles may correspond to magnesium-containing calcium carbonates, which have been observed to emit wide-spectrum fluorescence (Yoshida *et al*., 2010). Additionally, characteristic signals of calcium carbonate polymorphs, such as vaterite, monohydrocalcite, calcite, ikaite and aragonite, along with thenardite (Na_2SO_4, likely the result of high Na^+ and SO_4^{2-} in Salt Lake) and quartz (presumably from diatom frustules) were detected in the precipitates by micro-XRD (Fig. 5B).

Potential applications of urease field tests

The field detection of urease activity could prove useful for evaluating the predictability of fertilizer efficiency. Urea-based fertilizers are hydrolysed by soil bacteria, resulting in volatilization and nitrogen loss to the atmosphere, which is not utilized by crops (Cantarella *et al*., 2018; Modolo *et al*., 2018). Although not evaluated in this study, the use of a simple test that could be employed by farmers to determine on-site urease activity from soils may help decide appropriate fertilizer types for a given region (Ouyang and Norton, 2020), without the need of experienced personnel or laboratory equipment to perform the analysis. Although different laboratory assays intended to quantify soil urease activity are available (Kandeler and Gerber, 1988; Sinsabaugh *et al*., 2000; Cordero *et al*., 2019), they require several steps with hours-long incubations using different reagents and equipment (plate reader, centrifuge), making their implementation difficult – if not impossible – in the field. Field samples are transported, stored and analysed in a laboratory setting after days or weeks from their collection, which may result in urease activity changes derived from sample manipulation, temperature fluctuations, freeze–-thaw cycles and time until its analysis (Lee *et al*., 2007). By contrast, once assembled in microcentrifuge tubes, the rapid urease detection method provides a cheap and simple, one-step assay that could be carried out by inexperienced individuals, obtaining a qualitative result at the sampling site within minutes.

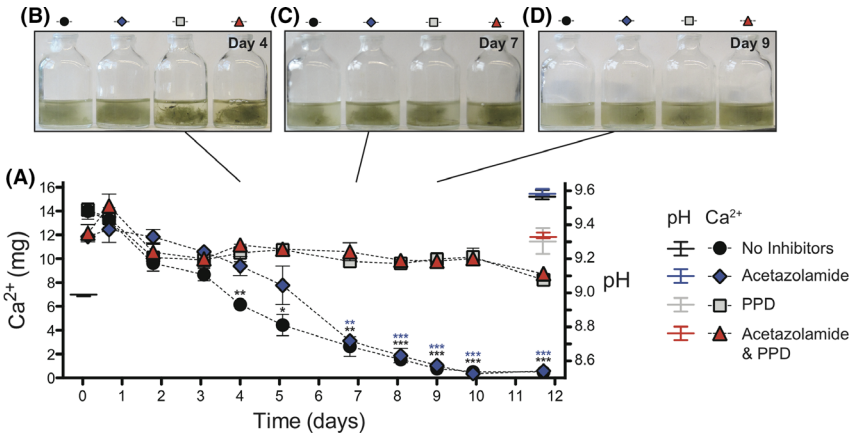

Fig. 4. Calcium depletion kinetics of Salt Lake water in the presence of its microbial biomass. (A) Calcium quantification (left axis) from aliquots taken over 12 days for triplicate incubations with a CA inhibitor (acetazolamide), a urease inhibitor (PPD) and conditions with and without both inhibitors. A pH increase (right axis) is observed at the end of the incubations. Standard error of triplicate assays is represented by the error bars, unless the error is smaller than the respective symbol. Bonferroni's *P*-values between each condition and the experiment with both inhibitors are shown with asterisks: *$0.1 < P < 0.05$, **$0.05 < P < 0.01$, ***$P < 0.01$. Photographs of representative incubations at Day 4 (B), 7 (C) and 9 (D) show hazy solutions attributable to mineral precipitation.

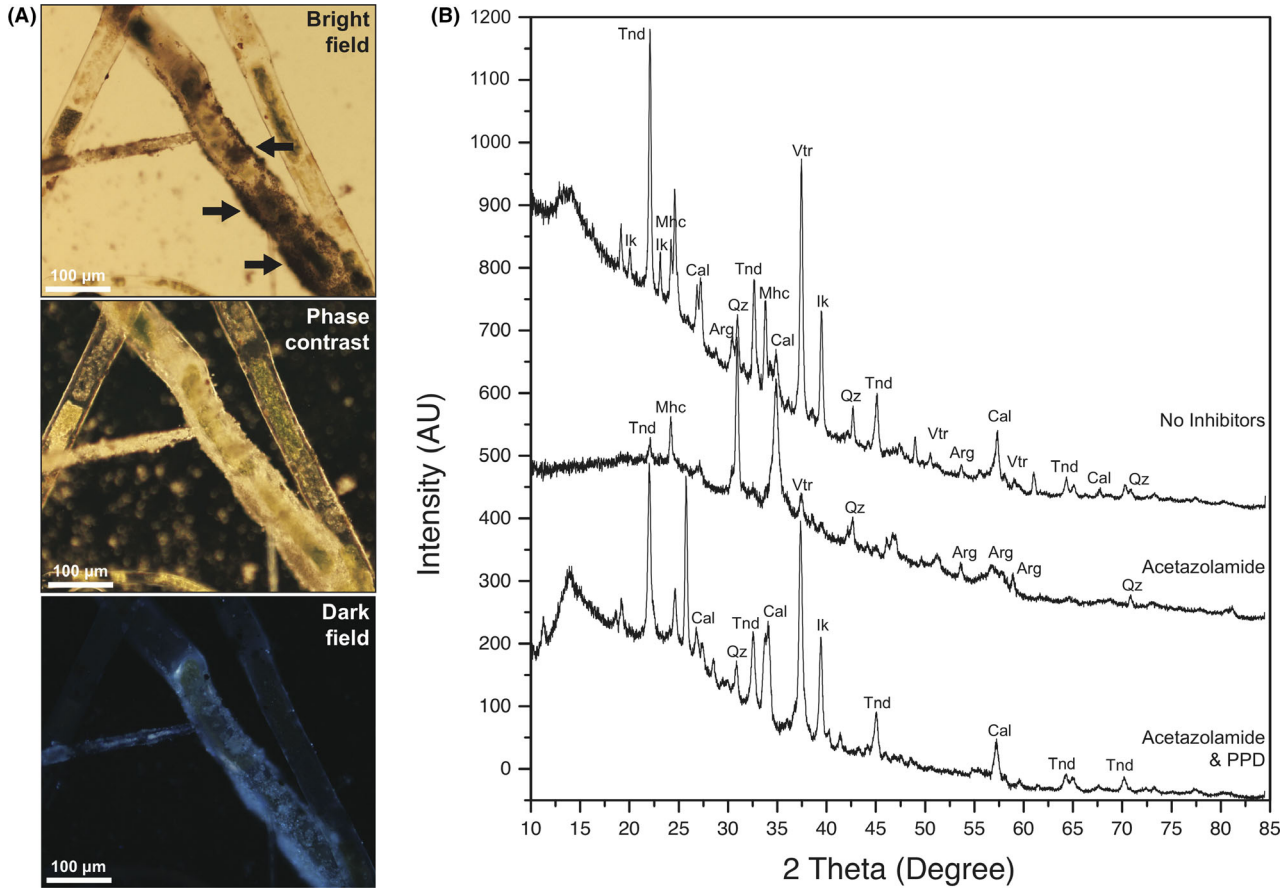

Fig. 5. Salt Lake microbial sheaths after incubations.
A. Filament photomicrographs after 12 days of incubation, showing black precipitates covering the sheaths under bright field (black arrows, top panel) that appeared white under phase contrast (middle panel) and have wide-spectrum autofluorescence (lower panel, dark field showing 420 nm-excited 450 nm long-pass emission).
B. Micro-XRD of precipitates after incubations without inhibitors, with acetazolamide and with both inhibitors. Mineral abbreviations: Arg, aragonite; Cal, calcite; Ik, ikaite; Mhc, monohydrocalcite; Qz, quartz; Tnd, thenardite; Vtr, vaterite.

The field test may also be useful for rapid and inexpensive screening of environmental organisms with high urease activity that can be used for engineering applications. Urease-driven MICP has been explored in recent years for cementation and restoration of diverse structures, from art sculptures to buildings, as well as bedrock plugging for enhanced oil recovery (Dhami *et al*., 2013; Krajewska, 2018). Application of ureolytic bacteria, however, requires evaluating the presence of urease activity, hopefully at the site of application, to provide evidence that the restoration approach is likely to work under the intended conditions. Rapid on-site evaluation of urease activity could help predict the efficiency of restoration approaches, instead of waiting for long-term reactive solutions.

A simple and economical test to detect enzymatic activity in the field may also help us understand the microbial processes that contribute to the chemistry and mineralogy of poorly studied sites. For example, though calcareous fens and other peatland ecosystems are extensive in some regions and are relevant carbon sinks (Lunt *et al*., 2019), little information exists about the activity of their microbial communities, in particular the activity of urease. We showed here not only that calcareous fen microbes have the potential to express urease, but also that their urease is active *in situ* in certain environments, where urease-driven MICP could occur. Though the increasing use of fertilizers has been linked to ecosystem damage, it may be possible to encourage the use of urea-based fertilizers in regions that are hydrologically connected to calcium-rich areas (such as calcareous fens) where indigenous microbes are known to drive MICP, resulting in a sustainable carbon sequestration alternative (Mitchell *et al*., 2010).

An economical test may be useful for educational demonstrations and also could prove valuable for determining temporal variations of environmental metabolisms along different seasons, days or even hours, which may otherwise prove difficult because of budget constraints. In-field tests may also be convenient to assess the influence of MICP on microbialites, particularly where bicarbonate transport and urease-related genes are known to be present (Warden *et al*., 2016), which could help us understand the elusive metabolisms involved in ancient microbialite formation (Bosak *et al*., 2007).

Top-down molecular studies of microbial communities and their environmental effects have exploded in the past decade, increasing our understanding of uncultivable microorganisms as well as the diversity of distinct environments in a microbe-dominated Earth. The information currently obtained via high-throughput sequencing of environmental microbes should be complemented with field activity assays to assess not only metabolic potential, but also microbial activity in a given environment. Enzymatic activities not only represent protein expression, but also the direct microbial effects on the environment, which in this study has been related to carbonate precipitation. We anticipate that field-based bottom-up approaches will aid in addressing challenging questions, such as determining the microbial role in mineral formation, as well as providing new eco-friendly technologies for engineering challenges. To our knowledge, this is the first field environmental urease and CA evaluation using an inexpensive and fast method developed with conventional laboratory materials. We expect that a variety of other environments can be tested using this method by other researchers, expanding our knowledge of environmental protein expression and its effects on MICP.

Experimental procedures

Rapid urease field test

Urease activity was evaluated using a modification of the rapid urease test for the detection of *Helicobacter pylori* in clinical samples (Thillainayagam *et al*., 1991; Ross and Behar, 2012). The test consists of a sample-loading strip containing urea (urease substrate) and a pH-sensitive indicator strip. Sample-loading strips were prepared by immersing a cellulose fibre sheet paper P8 (Thermo Fisher Scientific, Cat. 09-795D, Waltham, MA, USA) in a fresh 0.6 M urea, 0.4 mM EDTA solution (50 ml per 100 cm^2 of paper sheet) using a rocking flat glass pan to impregnate the paper thoroughly for 30 s per side. The impregnated paper sheet was extended on a tilted (~45°) dry flat glass surface to drain excess solution and left drying at room temperature (~10 h). Indicator strips were similarly prepared by impregnating a paper with fresh 0.02 % phenol red solution adjusted to pH 6.0 with 50 mM HCl. After the papers dry completely, circles of 6.5 mm diameter (or alternatively, strips of 4×8 mm) were cut from both the urea- and indicator-impregnated papers.

To assemble the test, individual sample-loading strips were introduced in Seal-Rite 0.5 ml microcentrifuge tubes (USA Scientific, Ocala, FL, USA), and indicator strips were placed inside the seals of the caps (Fig. 1A). Urease activity was detected by adding standard solutions of urease from *Canavalia ensiformis* (one unit, U, was defined as the quantity of enzyme that liberates 1 μmole of ammonia from urea per minute at pH 7.0 and 25°C; product number U1875, Sigma-Aldrich, St. Louis, MO, USA) or wet biofilm samples in direct contact with the sample-loading strip before tightly closing the tube. A positive reaction was visualized by a colour change from yellow to red in the indicator strip after ~ 5–60 min of incubation at room/field temperature (Fig. 1B). Volatile ammonia released from urea (Eq. 1) increases the pH in the

indicator strip, changing its colour (Fig. 1C). During the test, it is important to prevent any contact of the sample with the indicator strip to avoid a colour change derived from alkaline or acidic samples that may turn the indicator. The dry format of this test yields a faster reaction compared to other liquid- or gel-based assays (Tseng *et al*., 2005) and makes it conducive to field deployment.

A negative control was prepared under the same conditions and additionally adding 1 mM phenyl phosphorodiamidate (PPD) – a urease inhibitor – in the soaking solution of sample-loading strips. A positive reaction without the inhibitor and a negative reaction with PPD strongly indicate urease activity. The test, prepared as described here in closed microcentrifuge tubes, lasts at least one year stored at room temperature and protected from light with no decrease in sensitivity. The negative control containing PPD, however, expires after ~ 2–-3 months, because the PPD inhibitor is sensitive to oxygen. After three months, the PPD-impregnated strips are unable to inhibit high urease concentrations and may result in a false positive reaction, although yielding a considerably less intense colour change than the urease test without inhibitor. We recommend preparing the inhibitor-impregnated loading strips from a fresh PPD solution a few days prior to use, or alternatively, storing the loading strips under anoxic conditions and protected from light.

Rapid CA field test

CA assays were based on a CO_2 detection strip intended for proper endotracheal catheter introduction (Fehder, 1988). CO_2-sensitive strips were prepared, similarly to the urease field test strips, by soaking a cellulose fibre paper grade P8 (Thermo Fisher Scientific, Cat. 09-795D, Waltham, MA, USA) with a fresh solution containing 0.0065 M Na_2CO_3, 0.01% metacresol purple and 50% glycerol diluted with N_2-purged distilled water. Impregnated papers were immediately dried on a flat glass surface by a stream of hot air (~ 15 min), and circles of 6.5 mm (or strips of 4×8 mm) were cut and placed inside the cap seals of 0.5 ml microcentrifuge tubes (USA Scientific, Ocala, FL, USA; Fig. 1D). Inside microcentrifuge tubes, the bluish-purple indicator gradually turns purplish-yellow after three days of exposure to atmospheric CO_2, which limits the extent of using this method for field applications. We recommend using indicator strips prepared no more than 2 days in advance.

CA activity was detected by introducing 80 μl of cold 1 M $NaHCO_3$ in the tubes and immediately adding the samples, or 15 μl of standard CA (isozyme II from bovine erythrocytes; Sigma-Aldrich, St. Louis, MO, USA) solutions. The tubes were immediately closed and incubated on ice. Bicarbonate dehydration (catalysed by CA, Eq. 2) produces volatile CO_2, which reacts with glycerol-absorbed water in the indicator lid and generates acidity that turns the indicator from bluish-purple to purplish-yellow (Fig. 1E). Non-enzymatic bicarbonate dehydration proceeds rapidly, and therefore, the indicator colour change is observed within minutes, even without the enzyme. For this reason, it is important to use cold solutions and incubate the assay tubes on ice. Cold incubation limits non-enzymatic CO_2 hydration to a larger degree than the CA-mediated reaction and is essential for visualizing a reaction time difference between negative controls and CA-incubated reactions. Wilbur and Anderson (1948) noted the utility of cold incubations, which has since been applied in most CA hydratase activity assays to date. By using the CO_2-sensitive strips in microcentrifuge tubes, we found a subtle, but reproducible, colour change difference between CA-incubated (15–85 mM CA) and negative controls assayed simultaneously. Negative controls were prepared under the same conditions and adding 5 μl of fresh 1 mM acetazolamide – a CA inhibitor – to the bicarbonate buffer. A faster colour change compared to negative controls is indicative of CA activity.

Microbial sampling locations

Samples were taken near calcareous fens in the Minnesota River Basin, from ferrous springs and from Salt Lake, MN, during July and August 2019 (see detailed locations in Fig. S2 and Table S1). Salt Lake is an alkaline sulphate- and sodium-dominated saline lake. The lake alkalinity (234 ± 2 mg l^{-1} $CaCO_3$, pH 8–9), together with calcium carbonates in its sediments (Dean *et al*., 1993), indicates favourable conditions for carbonate mineral precipitation, which could be stimulated by microbial metabolisms. A sample of buoyant green biomass was collected from Salt Lake during a bloom event in July 2019. Submerged green filaments attached to shoreland rushes were also collected following the bloom in August 2019 (Fig. S3).

Calcareous fens, peatlands in which surficial calcium carbonate precipitates (Almendinger and Leete, 1998), are also environments where microorganisms may contribute to carbonate mineralization. Samples were collected from green biofilms growing on peat exposed by a creek at Black Dog Lake Fen, and from surficial green filaments suspended on water ponds during flood events in Nicols Meadow Fen, and between Fortier 8 Fen and Sioux Nation WMA Fen (locations shown in Table S1 and Fig. S4). Additionally, samples from iron-oxidizing microbes were collected from orange precipitates at a creek in Nicols Meadow Fen, from groundwater seeping to the Mississippi River at Saint Mary's Spring and from a sulphide seep at a roadside near Soudan, MN

(Fig. S5). A small portion of biomass (enough to wet the sample-loading strip of the urease assay) was evaluated on-site in triplicate (with the exception of the Salt Lake bloom sample, where only two samples were evaluated) for urease and CA activity using the rapid field test. Additional triplicate aliquots for each sample were obtained for protein extraction and microscopic observations (see detailed extraction methods in the supplementary file).

Calcium depletion kinetics

Salt Lake filaments (Sample ID 02 in Table S1) were incubated (0.5 g wet weight) in 20 ml of 0.2 μm-filtered lake water with the addition of 0.8 M urea in closed 50-ml glass serum bottles with agitation (90 r.p.m., orbital shaker MaxQTM 2000, Thermo Fisher Scientific) at room temperature and under natural light cycles for 12 days. Four different incubation conditions were evaluated in triplicate: lake water without inhibitors, lake water with 1 mM acetazolamide, lake water with 1 mM PPD and lake water with both inhibitors (1 mM each). Aliquots of 0.5 ml were taken over time and titrated with EDTA (HAC-DT, Hach, Loveland, CO, USA) to quantify calcium. Solid residues after incubations were evaluated by powder micro X-ray diffraction (micro-XRD) using a Bruker D8 Discover microdiffractometer with a CoKα source ($\lambda = 1.78899$ Å) equipped with a graphite monochromator and a 2D Vantec 500 detector. Samples were mounted on vacuum grease, and three frames (30° 2θ width) centred at 20°, 45° and 70° were collected for 900 s at 40 kV and 35 mA. Phase identification was conducted using Match! (v3.8.3.151) and the Crystallographic Open Database (COD-Inorg REV218120 2019.09.10) reference patterns for aragonite (96-901-6601), calcite (96-900-0971), monohydrocalcite (96-901-2074), quartz (96-901-0145), thenardite (96-900-4093) and vaterite (96-150-8972). Ikaite diffraction pattern was obtained from Hesse *et al*. (1983).

Image and statistical analysis

To compare and semi-quantify the rapid test results, we followed colour changes using hue values. The hue represents colour pigmentation by a single number, disregarding saturation and brightness, therefore, minimizing colour differences resulting from light and exposure time changes in the field (Fig. S9). Average hue values were calculated from RGB colours of standard circle areas over photographs of the indicator strips using the NIH ImageJ 1.49v software. Statistical significance of hue values from the rapid assays was assessed via mixed-effects models (considering the reaction time, as well as the presence or absence of inhibitor for each site, as nominal variables) with Geisser-Greenhouse correction using GraphPad Prism 8.3.0. Differences between each assay at a given incubation time and its respective control containing an enzyme inhibitor were evaluated by Bonferroni's multiple comparisons tests. Statistical analysis for the calcium depletion kinetic experiments was similarly evaluated via a two-way ANOVA and Bonferroni correction to compare between experimental conditions.

Acknowledgement

We thank Michael Rosen, Matt Oberhelman, Kim Lapakko, Beverly Flood, Javier García Barriocanal and Barbara MacGregor for field/laboratory support and discussions. We also thank the anonymous reviewers for helpful suggestions to improve the quality of this manuscript. The authors declare no conflict of interest. Parts of this work were carried out in the Characterization Facility, University of Minnesota, which receives partial support from NSF through the MRSEC program. This research was funded by a NASA award NNX14AK20G to JVB. FMF acknowledges the UMN Graduate School DDF, Fulbright 15150776 and CONICYT folio-72160214 fellowships. KH was supported by a MnDRIVE Environment initiative grant at the University of Minnesota.

Conflict of interest

None declared.

REFERENCES

Achal, V., and Pan, X. (2011) Characterization of urease and carbonic anhydrase producing bacteria and their role in calcite precipitation. *Curr Microbiol* **62:** 894–902.

Almendinger, J.E., and Leete, J.H. (1998) Peat characteristics and groundwater geochemistry of calcareous fens in the Minnesota River Basin, U.S.A. *Biogeochemistry* **43:** 25.

Amtul, Z., Rahman, A.-U., Siddiqui, R.A., and Choudhary, M.I. (2002) Chemistry and mechanism of urease inhibition. *Curr Med Chem* **9:** 1323–1348.

Baliukynas, M., Veteikytė, A., Kairys, V., and Matijošytė, I. (2020) The hydrolysis of indoxyl acetate: A versatile reaction to assay carbonic anhydrase activity by high-throughput screening. *Enzyme Microb Technol* **139:** 109584.

Bosak, T., Greene, S.E., and Newman, D.K. (2007) A likely role for anoxygenic photosynthetic microbes in the formation of ancient stromatolites. *Geobiology* **5:** 119–126.

Bose, H., and Satyanarayana, T. (2017) Microbial carbonic anhydrases in biomimetic carbon sequestration for mitigating global warming: prospects and perspectives. *Front Microbiol* **8:** 1615.

Cantarella, H., Otto, R., Soares, J.R., and de Silva, A.G.B. (2018) Agronomic efficiency of NBPT as a urease inhibitor: a review. *J Adv Res* **13:** 19–27.

Cordero, I., Snell, H., and Bardgett, R.D. (2019) High throughput method for measuring urease activity in soil. *Soil Biol Biochem* **134:** 72–77.

Dean, W.E., Gorham, E., and Swaine, D.J. (1993) Geochemistry of surface sediments of Minnesota Lakes. In *Elk Lake, Minnesota: Evidence for Rapid Climate Change in the North-Central United States*. Geological Society of America Special Paper. Boulder, CO: Geological Society of America, pp. 115–133.

Dhami, N.K., Reddy, M.S., and Mukherjee, A. (2013) Biomineralization of calcium carbonates and their engineered applications: a review. *Front Microbiol* **4:** 314.

Dhami, N.K., Reddy, M.S., and Mukherjee, A. (2014) Synergistic role of bacterial urease and carbonic anhydrase in carbonate mineralization. *Appl Biochem Biotechnol* **172:** 2552–2561.

Fehder, C.G. (1988) Carbon dioxide indicator device. US4728499A.

Glibert, P.M., Maranger, R., Sobota, D.J., and Bouwman, L. (2014) The Haber Bosch-Harmful Algal Bloom (HB-HAB) Link. *Environ Res Lett* **9:** 105001.

Hesse, K.-F., Küppers, H., and Suess, E. (1983) Refinement of the structure of Ikaite, $CaCO_3{\cdot}6H_2O$. *Z Krist-Cryst Mater* **163:** 227–231.

Innocenti, A., and Supuran, C.T. (2010) Paraoxon, 4-nitrophenyl phosphate and acetate are substrates of α- but not of β-, γ- and ζ-carbonic anhydrases. *Bioorg Med Chem Lett* **20:** 6208–6212.

Kafarski, P., and Talma, M. (2018) Recent advances in design of new urease inhibitors: A review. *J Adv Res* **13:** 101–112.

Kandeler, E., and Gerber, H. (1988) Short-term assay of soil urease activity using colorimetric determination of ammonium. *Biol Fert Soils* **6:** 68–72.

Krajewska, B. (2018) Urease-aided calcium carbonate mineralization for engineering applications: A review. *J Adv Res* **13:** 59–67.

Krausfeldt, L.E., Farmer, A.T., Castro Gonzalez, H.F., Zepernick, B.N., Campagna, S.R., and Wilhelm, S.W. (2019) Urea is both a carbon and nitrogen source for *Microcystis aeruginosa*: tracking ^{13}C incorporation at bloom pH conditions. *Front Microbiol* **10:** 1064.

Kumar, R.S.S., and Ferry, J.G. (2014) Prokaryotic carbonic anhydrases of Earth's environment. *Subcell Biochem* **75:** 77–87.

Lee, Y.B., Lorenz, N., Dick, L.K., and Dick, R.P. (2007) Cold storage and pretreatment incubation effects on soil microbial properties. *Soil Sci Soc Am J* **71:** 1299.

Li, Q., Csetenyi, L., Paton, G.I., and Gadd, G.M. (2015) $CaCO_3$ and $SrCO_3$ bioprecipitation by fungi isolated from calcareous soil. *Environ Microbiol* **17:** 3082–3097.

Lunt, P.H., Fyfe, R.M., and Tappin, A.D. (2019) Role of recent climate change on carbon sequestration in peatland systems. *Sci Total Environ* **667:** 348–358.

Mitchell, A.C., Dideriksen, K., Spangler, L.H., Cunningham, A.B., and Gerlach, R. (2010) Microbially enhanced carbon capture and storage by mineral-trapping and solubility-trapping. *Environ Sci Technol* **44:** 5270–5276.

Mobley, H.L., Island, M.D., and Hausinger, R.P. (1995) Molecular biology of microbial ureases. *Microbiol Rev* **59:** 451–480.

Modolo, L.V., da Silva, C.J., Brandão, D.S., and Chaves, I.S. (2018) A minireview on what we have learned about urease inhibitors of agricultural interest since mid-2000s. *J Adv Res* **13:** 29–37.

Ouyang, Y., and Norton, J.M. (2020) Short-term nitrogen fertilization affects microbial community composition and nitrogen mineralization functions in an agricultural soil. *Appl Environ Microbiol* **86:** e02278-19.

Paerl, H.W., Scott, J.T., McCarthy, M.J., Newell, S.E., Gardner, W.S., Havens, K.E., *et al*. (2016) It takes two to tango: when and where dual nutrient (N & P) reductions are needed to protect lakes and downstream ecosystems. *Environ Sci Technol* **50:** 10805–10813.

Reeksting, B.J., Hoffmann, T.D., Tan, L., Paine, K., and Gebhard, S. (2020) In-depth profiling of calcite precipitation by environmental bacteria reveals fundamental mechanistic differences with relevance to application. *Appl Environ Microbiol* **86:** e02739-19.

Ross, P., and Behar, M. (2012) Test strip for h. pylori detection. US20120094371A1.

Sarayu, K., Iyer, N.R., and Murthy, A.R. (2014) Exploration on the biotechnological aspect of the ureolytic bacteria for the production of the cementitious materials–a review. *Appl Biochem Biotechnol* **172:** 2308–2323.

Seifan, M., and Berenjian, A. (2019) Microbially induced calcium carbonate precipitation: a widespread phenomenon in the biological world. *Appl Microbiol Biotechnol* **103:** 4693–4708.

Sinsabaugh, R.L., Reynolds, H., and Long, T.M. (2000) Rapid assay for amidohydrolase (urease) activity in environmental samples. *Soil Biol Biochem* **32:** 2095–2097.

Thillainayagam, A.V., Arvind, A.S., Cook, R.S., Harrison, I.G., Tabaqchali, S., and Farthing, M.J. (1991) Diagnostic efficiency of an ultrarapid endoscopy room test for *Helicobacter pylori*. *Gut* **32:** 467–469.

Tseng, C.-A., Wang, W.-M., and Wu, D.-C. (2005) Comparison of the clinical feasibility of three rapid urease tests in the diagnosis of *Helicobacter pylori* infection. *Dig Dis Sci* **50:** 449–452.

Warden, J.G., Casaburi, G., Omelon, C.R., Bennett, P.C., Breecker, D.O., and Foster, J.S. (2016) Characterization of microbial mat microbiomes in the modern thrombolite ecosystem of Lake Clifton, Western Australia using shotgun metagenomics. *Front Microbiol* **7:** 1064.

Wilbur, K.M., and Anderson, N.G. (1948) Electrometric and colorimetric determination of carbonic anhydrase. *J Biol Chem* **176:** 147–154.

Yoshida, N., Higashimura, E., and Saeki, Y. (2010) Catalytic biomineralization of fluorescent calcite by the thermophilic bacterium *Geobacillus thermoglucosidasius*. *Appl Environ Microbiol* **76:** 7322–7327.

Zhou, Y., Zhang, X., Li, X., Jia, P., and Dai, R. (2019) Evaluation of changes in *Microcystis aeruginosa* growth and microcystin production by urea via transcriptomic surveys. *Sci Total Environ* **655:** 181–187.

Zhu, T., and Dittrich, M. (2016) Carbonate precipitation through microbial activities in natural environment, and their potential in biotechnology: a review. *Front Bioeng Biotechnol* **4:** 4.

Zimmerman, S.A., Innocenti, A., Casini, A., Ferry, J.G., Scozzafava, A., and Supuran, C.T. (2004) Carbonic anhydrase inhibitors. Inhibition of the prokariotic beta and gamma-class enzymes from Archaea with sulfonamides. *Bioorg Med Chem Lett* **14:** 6001–6006.

Zimmerman, S.A., Ferry, J.G., and Supuran, C.T. (2007) Inhibition of the archaeal beta-class (Cab) and gamma-class (Cam) carbonic anhydrases. *Curr Top Med Chem* **7:** 901–908.

Supporting information

Additional supporting information may be found online in the Supporting Information section at the end of the article.

Table S1. Description of the environmental samples obtained in this study.

Fig. S1. Urease and carbonic anhydrase standard assays. (A) Colorimetric response after 20, 60, and 120 minutes of urease reaction measured by the phenol-hypochlorite method using urease standards (1.5–31 mU) with or without a urease inhibitor (PPD). (B) CA hydratase response (time for pH drop from 8.3 to 6.3) based on the Wilbur and Anderson (1948) method of standard CA solutions (0.05–1.5 nM) with or without its inhibitor, acetazolamide. All conditions were assayed with six replicates. Error bars represent standard error (when not shown, the error is smaller than the symbols). The urease colorimetric response was analyzed by a mixed-effects model, and the CA time response was evaluated by a two-way ANOVA, where * $0.1 < P < 0.05$, ** $0.05 < P < 0.01$, and *** $P < 0.01$ between each condition and its respective negative control assessed by Bonferroni's multiple comparisons test.

Fig. S2. Microbial sampling sites. Highlighted contour of Minnesota, USA, indicating with green circles the location of known calcareous fens. Enlarged insets show the sampling locations (red circles) at the Southeastern shore of Salt Lake (A), at a roadside between Fortier 8 and Sioux Nation WMA calcareous fens (B), from a stream at Black Dog Lake Fen, a pond at Nicols Meadow Fen, and a creek between Nicols Meadow Fen and Black Dog Lake North Fen (C), at St. Mary's Springs near the West shore of the Mississippi River (D), and from a sulfidic seep roadside Highway 169, near Soudan, MN (E). Calcareous fen locations and water bodies were obtained from the Minnesota Department of Natural Resources. Topographic maps were obtained from the USGS National Geospatial Program, The National Map.

Fig. S3. Microbial biomass in Salt Lake, MN. Lake shore showing a bright green cyanobacterial bloom (A) sampled in July 2019 and its decline in August 2019 (B), where dark green microbial filaments at the lake shore were sampled instead. Insets show a close-up of the bloom and microfilaments sampled (left panels). Right panels show bright field photomicrographs of the sampled biomass with a merged fluorescence image (insets) of chlorophyll (red) and DAPI (blue) emission. Note that the bloom event in A is dominated by a cyanobacterium resembling *Microcystis* spp., whereas the sample taken after the bloom decline is dominated by large green trichome sheaths, probably *Microcoleus* spp., adorned with numerous photosynthetic diatoms.

Fig. S4. Microbial filaments at calcareous fens. Inundation ponds showing green surficial filaments with bubbles at Fortier-Sioux Nation Fens (A) and abundant filaments mixed with aquatic plants (*Spirodela* spp.) at Nicols Meadow fen (B). Green biofilms also colonize the peat exposed in a stream-eroded cliff at Black Dog Lake Fen (C). Insets show a close-up of the biomass sampled (left panels). Right panels show bright field photomicrographs for each sample, with insets of merged fluorescence images of chlorophyll red emission and blue fluorescence from DAPI.

Fig. S5. Microbial mats at ferrous seeps. Orange precipitates from a stream between Nicols Meadow Fen and Black Dog Lake North Fen (A), from St. Mary's Spring ferrous seeps (B), and from a sulfidic seep near Soudan, MN (C, field photo credit to Tanner Barnharst). Insets show a close-up of the orange precipitates and microbial mats sampled. Right panels show bright field and fluorescence microscopy (insets) of chlorophyll (red) and DAPI (blue) emission. Note the stalks of iron-oxidizing bacteria in A and B, and abundant cyanobacterial filaments in B and C.

Fig. S6. Land use near Salt Lake and Sioux Nation WMA Fen. Minnesota land cover classification maps around Salt Lake (A) and Sioux Nation-Fortier fens (B). Classifications according to 2013 Landsat and Lidar data (Rampi *et al.*, 2013). Note the abundance of agriculture areas near Salt Lake compared to the calcareous fens. Quadrants with nitrogen fertilizer (anhydrous ammonia and urea) application restrictions are based on vulnerable groundwater areas according to the Minnesota Department of Agriculture. Calcareous fen locations were obtained from the Minnesota Department of Natural Resources. South Dakota areas are represented by USGS satellite images, Geospatial Data Sources (2019).

Fig. S7. Urease and carbonic anhydrase activity from protein extracts. Urease activity using the Berthelot reaction method (A; Achal *et al.*, 2009) and CA activity after the Wilbur and Anderson (1948) assay (B). A total of 1 μg of protein extracts from Salt Lake filaments (02), Fortier-Sioux filaments (03), Black Dog peat green biofilm (04), Nicols Meadow filaments (05), Black Dog Lake North orange precipitates (06), mixed orange and green mats from St. Mary's Spring (08), and Soudan streamers (09) were used. None of the extracts were significantly higher than a blank assay (*$P < 0.01$, Welch's t-test), which is also observed using in-gel activity assays (C & D; De Luca *et al.*, 2015). A red band on a yellow background indicates urease activity (C), whereas a yellow band on a purple background indicates CA activity (D).

Fig. S8. Salt Lake carbonate speciation and carbonate mineral solubilities. Bicarbonate and carbonate concentration as a function of pH, considering the alkalinity (234 mg l^{-1} as CaCO3) and calcium concentration (16 mM) of Salt Lake. Assuming constant calcium and carbon concentrations, the saturation index (SI) for calcium carbonate minerals increases linearly from pH 9.0 (lake water pH) to 9.6 (pH at the end of microbial incubations without urease inhibitors). Note that above pH 9.6, all metastable calcium carbonate phases are saturated. Solubility values at 25 °C were obtained from Plummer and Busenberg (1982), Kralj and Brečević (1995), and Bischoff *et al.* (1993).

Fig. S9. Quantification of hue values. (A) Color wheel diagram showing the hue range of the carbonic anhydrase and urease tests. (B) Histograms of hue pixels for representative indicator strip (test tube caps) assays during the enzymatic reaction. The hue was expressed as the average value from assay photos over time.

